Subcellular localization and dimerization of APLP1 are strikingly different from APP and APLP2

Daniela Kaden[1], Philipp Voigt[2,*], Lisa-Marie Munter[1], Karolina D. Bobowski[1], Michael Schaefer[2,*] and Gerd Multhaup[1,‡]

[1]Institut für Chemie und Biochemie, Freie Universität Berlin, 14195 Berlin, Germany
[2]Molekulare Pharmakologie und Zellbiologie, Neurowissenschaftliches Forschungszentrum, Charité-Universitätsmedizin Berlin, 14195 Berlin, Germany
*Present address: Medizinische Fakultät der Universität Leipzig, Rudolf-Boehm-Institut für Pharmakologie und Toxikologie, 04107 Leipzig, Germany
‡Author for correspondence (e-mail: multhaup@chemie.fu-berlin.de)

Accepted 13 October 2008
Journal of Cell Science 122, 368-377 Published by The Company of Biologists 2009
doi:10.1242/jcs.034058

Summary

The molecular association between APP and its mammalian homologs has hardly been explored. In systematically addressing this issue, we show by live cell imaging that APLP1 mainly localizes to the cell surface, whereas APP and APLP2 are mostly found in intracellular compartments. Homo- and heterotypic cis interactions of APP family members could be detected by FRET and co-immunoprecipitation analysis and occur in a modular mode. Only APLP1 formed trans interactions, supporting the argument for a putative specific role of APLP1 in cell adhesion. Deletion mutants of APP family members revealed two highly conserved regions as important for the protein crosstalk. In particular, the N-terminal half of the ectodomain was crucial for APP and APLP2 interactions. By contrast, multimerization of APLP1 was only partially dependent on this domain but strongly on the C-terminal half of the ectodomain. We further observed that coexpression of APP with APLP1 or APLP2 leads to diminished generation of Aβ42. The current data suggest that this is due to the formation of heteromeric complexes, opening the way for novel therapeutic strategies targeting these complexes.

Supplementary material available online at
http://jcs.biologists.org/cgi/content/full/122/3/368/DC1

Key words: Amyloid precursor protein (APP), Amyloid precursor-like proteins (APLPs), Subcellular localization, Cis and trans dimerization, APP processing

Introduction

The amyloid beta (A4) precursor protein (APP) involved in Alzheimer's disease belongs to an evolutionarily conserved protein family with its orthologs APPL and APL-1 in *Drosophila* and *Caenorhabditis elegans*, respectively (Coulson et al., 1997; Daigle and Li, 1993; Rosen et al., 1989). Amyloid beta (A4) precursor-like proteins 1 and 2 (APLP1 and APLP2) have been identified as mammalian homologs of APP (Paliga et al., 1997; Wasco et al., 1992; Wasco et al., 1993).

Upon integration into the plasma membrane APP functions as a cell surface receptor, controlling adhesion and signaling (Atwood et al., 2000; Cao and Sudhof, 2001; Nishimoto et al., 1993; Shivers et al., 1988; Soba et al., 2005; Storey et al., 1996). APP and APLPs belong to a group of type I transmembrane proteins that includes Notch and sorting receptors Sortilin, SorCS1b, and SorLA (Nyborg et al., 2006), which participate in highly conserved processing pathways (Brunkan and Goate, 2005). Cleavage of APP and Notch by the γ-secretase liberates the corresponding intracellular domains, which exert nuclear signaling (Cao and Sudhof, 2001; Scheinfeld et al., 2002; Walsh et al., 2003). Aberrations in Notch signaling have been linked directly to several diseases in mammals, whereas processing of APP is the crucial step in the pathology of Alzheimer's disease. The processing product amyloid β peptide (Aβ), which is the main component of amyloid plaques, is exclusively derived from APP but not from other proteins.

Conventionally, APP and APLPs were thought to exist and act as monomers. However, there is accumulating evidence from biochemical and structural data that APP molecules may exist as dimers or even more complex oligomers (Chen et al., 2006; Rossjohn et al., 1999; Scheuermann et al., 2001; Wang and Ha, 2004). Interactions of APP and APLPs were reported to promote cell adhesion in a homo- and heterotypic manner (Soba et al., 2005). Among other mechanisms, the varying strength of APP dimerization was found to influence APP processing. Modulation of homotypic APP interactions in the E1 domain has been shown to impair APP cleavage by the APP β-site cleaving enzyme BACE (Kaden et al., 2008), whereas the transmembrane helix-helix interaction motif GxxxG has an important role for processing of Aβ42 and Aβ40 into even shorter Aβ species (Munter et al., 2007).

As little is known about the mechanisms by which APP and APLP domains are involved in homo- and hetero-oligomerization, we addressed this issue by live-cell imaging and biochemical approaches. We observed clearly distinct properties of the APP family members and found distinct domains to be involved in subcellular localization and cis and trans interactions. Furthermore, coexpression of APP with APLP1 or APLP2 led to a significantly diminished generation of the toxic Aβ42, implying that homo- and heterodimeric complexes are processed differently.

Results

Live-cell imaging of the APP family proteins

For a thorough analysis of APP, APLP1 and APLP2 homo- or heterotypic interactions we first determined the individual subcellular localization, because this controls access to and

Journal of Cell Science

availability of molecular interacting partners. We assessed the subcellular localization of APP family proteins in living HEK293 cells by confocal laser scanning microscopy (cLSM), using expression plasmids encoding APP, APLP1 or APLP2 C-terminally fused to the yellow or cyan fluorescent protein (YFP or CFP) (Fig. 1A). To distinguish between the intracellular compartments we used fluorescent marker proteins targeting ER, Golgi or endosomes and a lysosome-targeted dye. APP-YFP was mostly present in intracellular compartments such as the ER and endosomes and to a lesser extent in the Golgi apparatus, as determined by coexpression with the corresponding marker proteins (Fig. 1B, right panel; supplementary material Fig. S1A-D). Only a small fraction was detected at the plasma membrane. By contrast, APLP1-YFP was mainly localized to the cell surface (Fig. 1B, left panel), but also partly present in endosomal vesicles (supplementary material Fig. S1A-D). APLP2-YFP showed an almost equal distribution between the plasma membrane and intracellular compartments (Fig. 1B, middle). These were mostly endosomes, with a minor fraction residing in the ER and Golgi apparatus (supplementary material Fig. S1A-D). Interestingly, although all three proteins are homologous and are characterized by a conserved domain structure, they clearly exhibit distinct subcellular distributions.

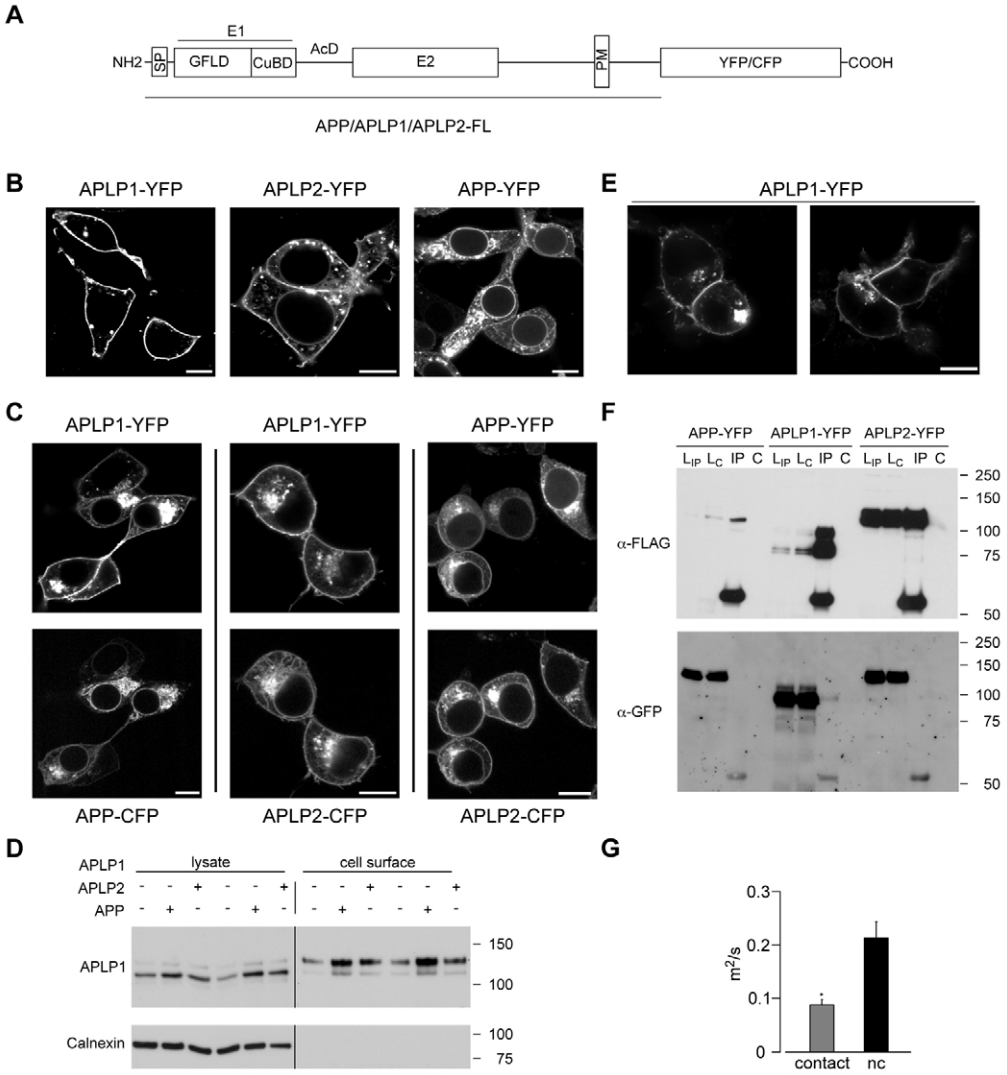

Fig. 1. Subcellular localization of APP family proteins. Human APLP1, APLP2 and APP full-length proteins were C-terminally fused to YFP or CFP. (A) Schematical view. The respective plasmids were transiently transfected in HEK293 cells either alone (B) or in combination with one of the other APP family members (C). Note that APLP1 accumulates in intracellular compartments when coexpressed with APP or APLP2 (C, first two panels compared to APLP1 alone). (D) Cell surface biotinylation of APLP1 upon APP and APLP2 coexpression. HEK293 cells were transiently co-transfected with the indicated constructs and cell surface proteins were labeled by sulfo-NHS-SS-biotin. Shown is the total (lysate) and the cell-surface-localized APLP1-YFP of two different transfections. Calnexin was used as a loading control and to verify the absence of endomembranes from biotinylation. Molecular weight standard is indicated on the right. APLP1 was stained with a polyclonal APLP1-specific antibody (42464). (E) APLP1-YFP is enriched in cell-cell contacts. Additional images are shown in supplementary material Fig. S4. (B,C,E) Cells were imaged by cLSM 1 day after transfection. Representative images of at least three independent transfections are shown. (F) Analysis of dimer/oligomer formation in trans direction. APP, APLP1 and APLP2 fused to either FLAG or YFP tags were expressed separately in HEK293 cells and then the cells were mixed 1 day before harvesting. Co-immunoprecipitations were carried out with the FLAG antibody and co-purified proteins were detected by GFP antibody. Molecular weight standard is indicated on the right. (G) Velocity of APLP1-YFP lateral plasma membrane diffusion was determined by FRAP analysis in areas of cell-cell contacts and non-contact sites. Bars, 10 µm. *, $P<0.001$, Wilcoxon test; C, control IP without antibody; FL, full-length; L_C, lysates from control; L_{IP}, lysates from IP; IP, immunoprecipitation with FLAG antibody; nc, non-contact sites; PM, plasma membrane; SP, signal peptide.

Journal of Cell Science

Journal of Cell Science

To verify that the subcellular distribution of APLP1 and APLP2 is not influenced by the YFP moiety, immunofluorescence analysis of fixed and permeabilized HEK293 cells was performed. Cells were transiently transfected with either YFP- or FLAG-tagged proteins. The FLAG-tagged proteins revealed the same localization pattern as the corresponding fluorescent fusion proteins (supplementary material Fig. S2). Taken together with results previously obtained for APP (Munter et al., 2007), we conclude that the localization of APP and APLPs remains unchanged by the fluorescent tag.

All possible pairings of APP and APLPs were assayed to investigate whether co-expression interferes with individually encoded sorting information. APP and APLP2 co-localized to a large degree in co-transfected cells in agreement with the overlapping localization patterns of APP or APLP2 in single transfected cells (Fig. 1B,C, right panels). Coexpression of APP-CFP and APLP1-YFP (or of APP-YFP and APLP1-CFP, data not shown) revealed a partial retention of APLP1 in the ER and Golgi compartments (Fig. 1C, left). Co-localization of APP and APLP1 at the plasma membrane was observed in only a few cells due to the typically low level of APP on the cell surface (Fig. 1B). Likewise, APLP1-YFP was partially retained in intracellular compartments when coexpressed with APLP2-CFP (Fig. 1C, middle). Even though APLP1 seems partially retained in intracellular compartments upon coexpression, there was still a high level of APLP1-YFP present at the plasma membrane. Western blot analysis revealed that the total amount of APLP1 in the lysate increased as well as the cell surface level, as determined by biotinylation (Fig. 1D). Apparently, APLP1 heterodimerization with APP or APLP2 may lead to stabilization of APLP1, especially in intracellular compartments, mimicking retention.

These results show that APP family proteins, and in particular APLP1, show distinct subcellular distributions and differ in their degree of cell surface localization. Both APP and APLP2 strongly retain and stabilize APLP1 in intracellular compartments, indicating that interactions between the APP family proteins may occur as early as in the ER.

APLP1 is involved in cell-cell contacts

Because APP family proteins have been implicated in cell adhesion (Beher et al., 1996; Small et al., 1994; Soba et al., 2005) and because we detected APLP1 at high levels at the cell surface, we examined a possible involvement of APLP1 in trans cell interactions in living cells (Fig. 1). Indeed, we found APLP1-YFP enriched at cell-cell contact sites (Fig. 1E), whereas such accumulations were not detectable for APP-YFP or APLP2-YFP (Fig. 1B) (see supplementary material Fig. S4 for additional images of all APP family proteins). To obtain further evidence for trans interactions of APLP1 we performed co-immunoprecipitation assays. HEK293 cells were separately transfected with APP/APLP-YFP or APP/APLP-FLAG, and YFP- and FLAG-tag-expressing cells were mixed one day before harvesting. We could detect only APLP1-YFP in FLAG-directed pull-downs, clearly demonstrating the occurrence of trans interactions (Fig. 1F, lane APLP1-YFP/IP). Neither APP-YFP nor APLP2-YFP were co-purified with the respective FLAG proteins, indicating that these two proteins are not involved in trans interactions in HEK293 cells (Fig. 1F). These data complement the results obtained by cLSM (Fig. 1B,E; supplementary material Fig. S4). If the APLP1 accumulation results from a structural network of cis and trans dimerization, the mobility of APLP1-YFP in the plasma membrane should be reduced at the contact site. Thus, to quantify the lateral diffusion of APLP1-YFP, we carried out a fluorescence recovery after photobleaching (FRAP) analysis. The velocity of APLP1-YFP molecules within the contacts was reduced by about 50% (Fig. 1G), indicating that trans interactions of APLP1 do occur. Control measurements were performed to verify that recovery occurs via lateral diffusion and not via exocytotic supply (see supplementary material Movies 1 and 2).

These results align the evident difference in subcellular localization of APLP1 compared with APP and APLP2 with a functional feature of APLP1 in mediating trans interactions at cell-cell contacts.

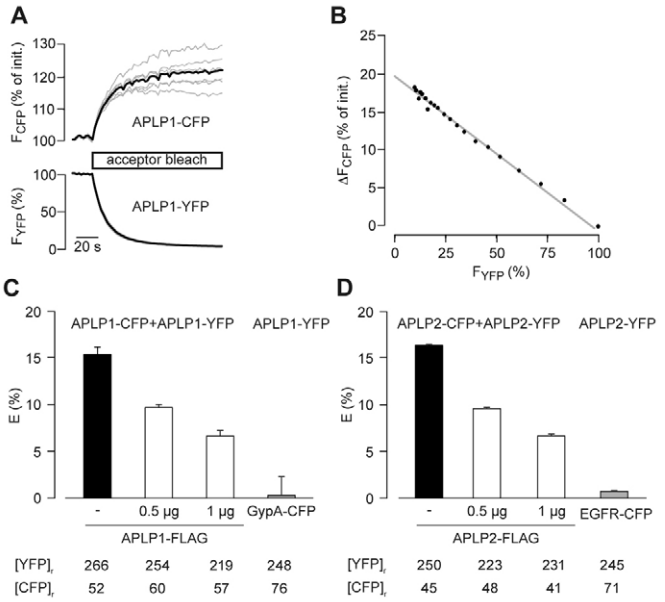

Fig. 2. Homodimerization of APLP1 and APLP2. FRET efficiencies (E) in transiently transfected HEK293 cells were determined by measuring the recovery of CFP fluorescence during YFP photobleaching. Cells were excited at 410 and 515 nm for CFP and YFP detection, respectively. YFP was bleached by illumination at 512 nm for 2.1 seconds in each acquisition cycle. (A) Timecourse of donor fluorescence recovery (ΔFCFP) during selective photobleaching of the acceptor (FYFP). Shown are single cells (gray lines) and mean fluorescence traces (black lines) of a representative measurement of APLP1-CFP and APLP1-YFP. (B) Linear regression analysis of donor recovery versus fractional acceptor photobleach to extrapolate the donor fluorescence in the absence of acceptor. Depicted is the mean of the experiment shown in A. (C,D) Black bars denote FRET efficiencies for APLP1-CFP and APLP1-YFP (C) as well as APLP2-CFP and APLP2-YFP (D). Open bars represent the same measurements but with increasing amounts of the respective FLAG-tagged fusion protein. As negative control APLP1-YFP was coexpressed with glycophorin A (GypA-CFP; C, gray bar) and APLP2-YFP was coexpressed with EGF-receptor-CFP (D, gray bar). Numbers represent the relative CFP and YFP fluorescence intensities in single cells expressing the respective fusion proteins that were determined and averaged ($[YFP]_r$ and $[CFP]_r$) to verify comparable protein expression. Depicted are the means and s.e.m. of three to four independent transfections (with four measurements each on four to six cells).

Homodimerization of APLPs

To assess and to quantify homophilic interactions, we analyzed fluorescence resonance energy transfer (FRET) between coexpressed CFP- and YFP-tagged APLP1 and APLP2 fusion proteins in HEK293 cells. FRET efficiencies were determined by measuring the donor recovery during selective photobleaching of the acceptor (Fig. 2A,B). Both APLP1 and APLP2 displayed a

Journal of Cell Science

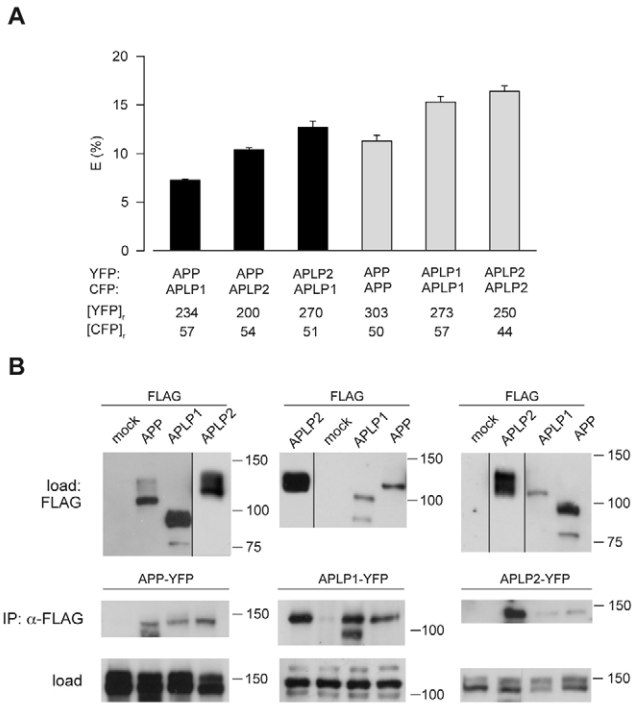

Fig. 3. Homo- and heteromultimerization of APP family proteins. (A) FRET analysis of human APP, APLP1, APLP2 hetero- (black bars) and homomultimerization (gray bars). YFP- and CFP-tagged fusion proteins were coexpressed in HEK293 cells in the indicated combinations. The relative CFP and YFP fluorescence intensities in single cells expressing the respective fusion proteins were determined and averaged ($[YFP]_r$ and $[CFP]_r$) to verify comparable protein expression. Depicted are means and s.e.m. of three independent transfections (n=4 with four to six cells each). Similar FRET efficiencies (E) were obtained if donor and acceptor were exchanged (data not shown). (B) Co-immunoprecipitations of human APP, APLP1 and APLP2. HEK293 cells were transfected with plasmids coding for FLAG-tagged APP, APLP1 and APLP2 and the corresponding YFP plasmids, as indicated. The FLAG fusion proteins were immunoprecipitated with anti-FLAG antibodies, and co-purified constructs were detected with protein-specific antibodies (IP: α-FLAG) 42464 for APLP1, 8/1 for APLP2 and W0-2 for APP. As loading control, cell lysates were analyzed with M2-FLAG monoclonal antibody (load: FLAG) and the protein-specific antibodies (load). Note, the YFP tag leads to a molecular weight shift of the detected YFP-tagged APP/APLP forms by about 25 kD.

FRET efficiency of about 16%, indicating the formation of homomultimers for both proteins in HEK293 cells (Fig. 2C,D). FRET signals originated from specific interactions between APLP molecules for the following reasons: (1) FRET efficiencies were reduced in the presence of increasing amounts of coexpressed non-fluorescent APLPs; (2) FRET efficiencies were negligible upon co-transfection with unrelated membrane proteins such as glycophorin A (GypA)-CFP (APLP1-YFP) (Fig. 2C) or EGF receptor-CFP (APLP2-YFP) (Fig. 2D). The latter two proteins were chosen as controls according to the subcellular localizations of the respective APLP protein. APP homodimers exhibit FRET efficiencies of about 11%, as we published earlier (Munter et al., 2007). Taking these results together, we conclude that all APP family members are able to homodimerize.

Heterodimerization of APP family proteins

The finding that APP expression strongly influenced APLP1 localization (Fig. 1B) indicated that heteromeric interactions may occur between APP family proteins. Thus, we applied the FRET approach to detect and quantify possible heteromeric assemblies of APP, APLP1 and APLP2. In HEK293 cells, which were transiently transfected with all pairings of YFP- or CFP-tagged APP and APLPs, significant FRET efficiencies were observed, indicating heterophilic interactions between all three APP family members (Fig. 3A). In agreement with the respective degree of co-localization, the FRET efficiencies for heterodimerization were lower for APP:APLP1 complexes (7.3±0.1%) but higher for the complexes APLP1:APLP2 (12.7±0.6%) and APP:APLP2 (10.4±0.2%) (Fig. 3).

To confirm the existence of homo- and heterophilic interactions between APP family members in HEK293 cells by an independent approach, co-immunoprecipitation analysis was performed. To this end, YFP-fused proteins were coexpressed with C-terminally FLAG-tagged proteins. By applying anti-FLAG antibodies, we could successfully co-purify the respective fluorescent fusion protein and thus confirm the presence of all possible homo- and heteromultimeric APP or APLP complexes (Fig. 3B). Note that SDS-resistant homodimers of APLP1-YFP and APLP2-YFP were detected by western blot analysis (supplementary material Fig. S3). With these results, we conclude that all APP family members can undergo both homo- and heteromultimerization in higher eukaryotic cells.

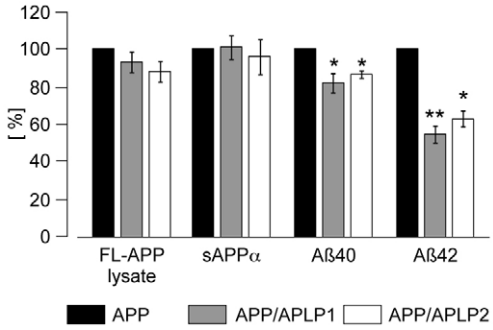

Fig. 4. Analysis of APP processing by sandwich ELISA under conditions of APLP coexpression. Full-length APP (FL-APP lysate) from lysates of APP-transfected cells or sAPPα from conditioned media were captured using an anti-Myc antibody and detected by biotinylated W0-2. Aβ40 and Aβ42 were captured using specific C-terminal antibodies and detected by biotinylated W0-2. The respective control was set as 100% (black bars) (means ±s.e.m., n=3-5; gray bars indicate APLP1/APP, white bars APLP2/APP co-transfections). Asterisks indicate significant differences to control (*P<0.05 and **P<0.005, Student's t-test).

Impact of APLP coexpression on APP processing

All APP family members are substrates of the same proteases, i.e. α-, β- and γ-secretases (Eggert et al., 2004; Li and Sudhof, 2004; Pastorino et al., 2004; Scheinfeld et al., 2002; Walsh et al., 2003). Therefore we examined whether the coexpression of APP with APLP1 or APLP2 can influence the processing of APP and thus Aβ generation. To this end, Aβ was quantified by ELISA from SH-SY5Y cells stably overexpressing APP in the presence and absence of APLP1 or APLP2. Comparable expression levels of APP between control, APLP1- and APLP2-transfected cells were verified by determining the amount of the overexpressed APP by ELISA (Fig. 4). Whereas sAPPα levels were found unchanged in these cells (Fig. 4), we detected a slight but significant decrease in Aβ40 species (18±5% for APLP1 and 13±2% for APLP2) and, strikingly, a drastic reduction of Aβ42 levels (45±5% for APLP1 and 37±4%

for APLP2) (Fig. 4). These data show that coexpression of APP with its homologs influences the processing of APP, resulting in a lower production of the toxic Aβ42 species.

Dissection of domains involved in homo- and heteromultimerization

The APP ectodomain bears two conserved regions, denoted E1 and E2 (Fig. 5A) (see also Daigle and Li, 1993). The E1 domain (Fig. 5A) contains two independent folding units, the growth factor-like domain (GFLD) and the copper-binding domain (CuBD) (Barnham et al., 2003; Rossjohn et al., 1999; Small et al., 1994). The so-called loop region is part of the GFLD and is involved in the structuring of APP (Kaden et al., 2008; Rossjohn et al., 1999; Scheuermann et al., 2001). The E2 domain (Fig. 5A) contains a second site that has been assumed to mediate homodimerization (Beher et al., 1996; Wang and Ha, 2004). The linker region between E1 and E2 is an acidic stretch (AcD) and is not well conserved between the members of the APP family. Nonetheless, it may have functions in modulating homo- and heteromultimerization, as it has a stabilizing function for APP dimers (Kaden et al., 2008). To dissect the contribution of the most N-terminal domains in cis oligomerization of APP and APLPs in a cellular environment, we generated the deletion mutants ΔGFLD, ΔE1 and ΔE1-AcD (Fig. 5A).

To assess the expression and correct localization of the C-terminally YFP-tagged deletion mutants, we analyzed them by cLSM (Fig. 5B; supplementary material Fig. S5) and western blot (supplementary material Fig. S6). All deletion mutants were expressed and located like the corresponding wild-type proteins (Fig. 5B; supplementary material Fig. S5). Only the APP-ΔE1-AcD encoded protein exhibited a slightly higher cell surface expression than wild-type APP (Fig. 5B; supplementary material Fig. S5). Because evaluation of the FRET determinations is based on total cellular fluorescence, the change in cell surface expression should not significantly influence the resulting FRET efficiencies. Surprisingly, FRET analysis revealed that the N-terminal domains of individual APP family proteins differentially influenced their multimerization. The GFLDs of APP and APLP2 are crucial for their homodimerization, as is evident from the diminished FRET efficiencies of the ΔGFLD mutants (Fig. 5C). By contrast, deletion of the corresponding region in APLP1 only marginally affects dimerization (Fig. 5C, middle). Whereas the shorter deletion mutants of APP (ΔE1 and ΔE1-AcD) and APLP2 (ΔE1-AcD) failed

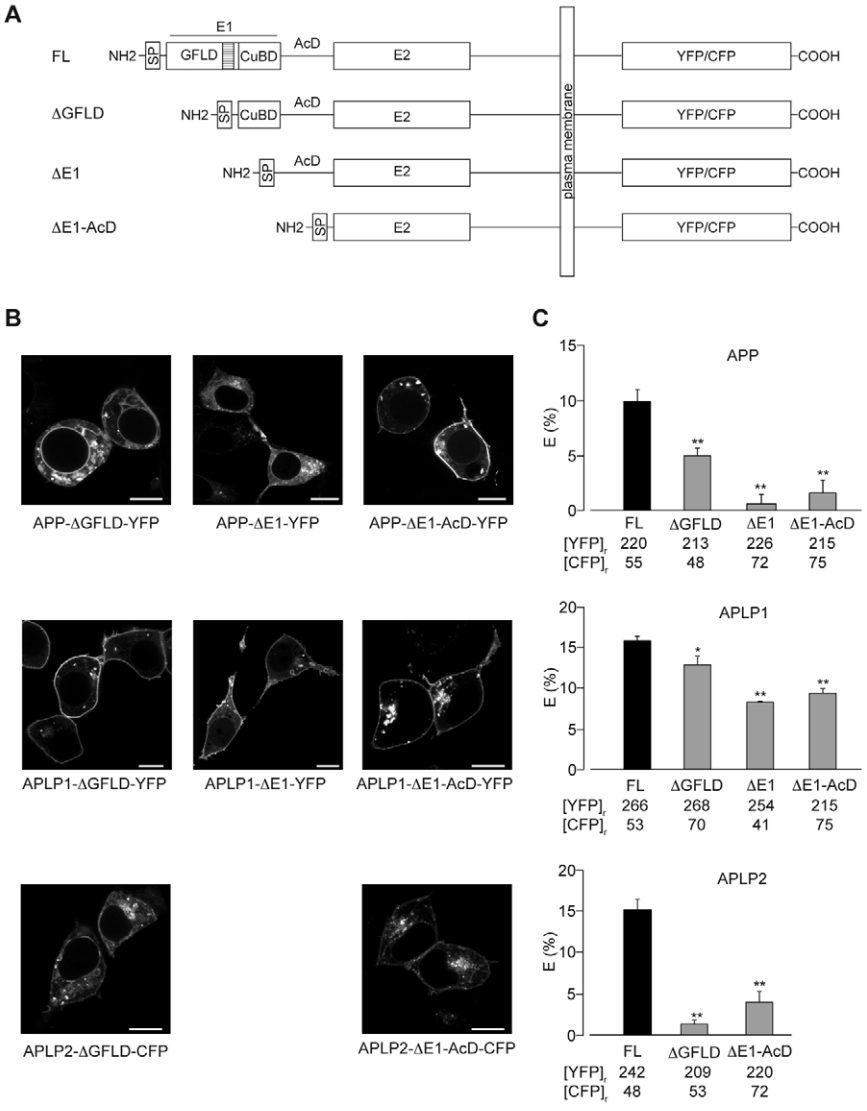

Fig. 5. Fluorescence imaging of N-terminal deletion mutants. (A) Schematic representation of N-terminal deletion mutants. For all deletion constructs the signal peptide sequence of APP was introduced in frame with the remaining domains. (B) Confocal imaging of the N-terminal deletion mutants. Either YFP- or CFP-tagged mutants were expressed in HEK293 and cells were imaged by cLSM 1 day after transfection. Representative images from at least three independent transfections are shown. For coexpression with the corresponding wild-type constructs see supplementary material Fig. S5. (C) Analysis of homointeractions of N-terminal deletion mutants in comparison to FL forms. The YFP- and CFP-fusion proteins were expressed in HEK293 cells and analyzed by FRET. The relative CFP and YFP fluorescence intensities in single cells expressing the respective fusion proteins were determined and averaged ($[YFP]_r$ and $[CFP]_r$) to verify comparable protein expression. Depicted are the means and s.e.m. of three to four independent transfections (with four measurements each on three to five cells). Bars, 10 µm. Striped square: loop region. *P<0.05, **P<0.001, Student's t-test. FL, full-length.

Journal of Cell Science

to exhibit homophilic interactions, deletion of these domains in APLP1 (ΔE1 and ΔE1-AcD) led only to about a 50% decrease in FRET efficiencies, demonstrating that these APLP1 deletion mutants still form homomeric assemblies (Fig. 5C, middle). These results suggest that other domains in addition to E1 are involved in mediating interactions of APLP1. Therefore, the mechanism of APLP1 homodimerization seems to differ significantly from that of APP or APLP2.

To verify this assumption and to further investigate the impact of the domains on cis interactions, the formation of heteromultimers between the full-length (FL) proteins and APP or APLP1 deletion mutants was analyzed by determining the FRET efficiencies. As observed for the homomeric assembly of APP, formation of heteromultimers with FL APLP1 and APLP2 was strongly dependent on the APP GFLD (Fig. 6A). By contrast, heterophilic interactions of APLP1 deletion mutants with FL APP or APLP2 were almost independent of the APLP1 GFLD, evidenced by minor changes in FRET efficiencies (Fig. 6B). This further corroborates the results obtained for APLP1 homomultimers. We conclude that the APP GFLD is essential not only for homophilic interactions but also for heterophilic interactions, whereas the APLP1 GFLD is dispensable for both homo- and heteromultimerization.

Deletion of the whole E1 domain of APLP1 (APLP1-ΔE1) led to a significant decrease in heteromeric interactions with APP or APLP2 (Fig. 6B). Interestingly, the extended deletion as represented by the APLP1-ΔE1-AcD mutant yielded a small rescue of FRET efficiencies up to the level of the ΔGFLD mutants (Fig. 6B). This suggests that the ΔE1 mutant although stably expressed might be structurally impaired and therefore shows a lower tendency to form heteromultimers than the deletion mutant ΔE1-AcD.

Taking these results together, we identified the GFLD as an essential domain in mediating the homo- and heteromeric assembly of APP and APLP2 molecules. By contrast, the contribution of the GFLD to homo- and heterophilic interactions appears to be much less pronounced for APLP1. Furthermore, multimerization of APLP1 was only partially dependent on the whole E1 domain. Therefore we conclude that the E2 domain and/or more C-terminal sequences might have a stronger impact on homo- and heterodimerization of APLP1 than of APP or APLP2.

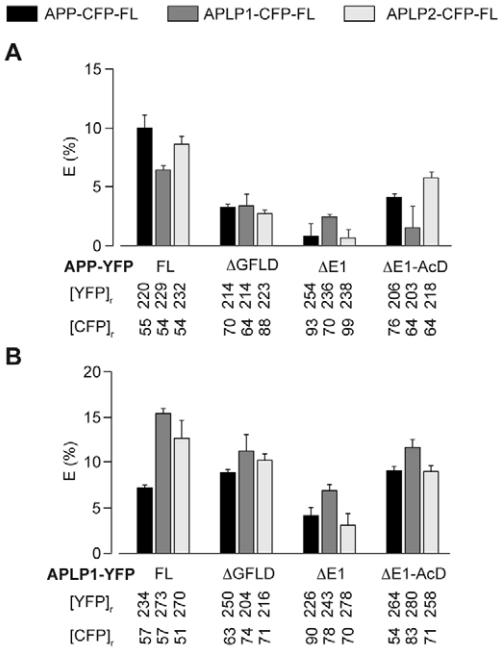

Fig. 6. Heteromultimerization analysis of N-terminal deletion mutants with full-length APP family members. Either full-length variants or the deletion mutants ΔGFLD, ΔE1 and ΔE1-AcD of APP (A) and APLP1 (B) were coexpressed with the corresponding FL protein and analyzed by FRET. Black bars indicate coexpression with APP-FL, dark gray bars with APLP1-FL and light gray bars with APLP2-FL proteins. The relative CFP and YFP fluorescence intensities in single cells expressing the respective fusion proteins were determined and averaged ($[YFP]_r$ and $[CFP]_r$) to verify comparable protein expression. Depicted are the means and s.e.m. of three to four independent transfections (with four measurements each on three to five cells). FL, full-length.

The disulfide loop of APP is important for multimerization

The results of this study together with previously reported findings (Kaden et al., 2008; Munter et al., 2007; Rossjohn et al., 1999; Scheuermann et al., 2001) indicate that the GFLD is important to stabilize conformations that support homo- and heterophilic interactions of APP and APLP2 but not of APLP1 (Figs 5 and 6). Based on findings that a synthetic peptide corresponding to the loop residues containing the conserved disulfide bridge between cysteines 98 and 105 of APP was able to interfere with APP dimerization (Kaden et al., 2008), we studied the role of these residues for homo- and heterophilic APP interactions. To determine whether the conformation of the loop formed by the cysteines 98 and 105 is crucial for APP N-terminal interactions, we generated single and double mutants APP loop-S1, loop-S2 and loop-SD, exchanging the cysteine with serine residues, and analyzed them in living cells (Fig. 7A).

Surprisingly, single and double mutants showed a reduced cell surface localization compared with wild-type APP accompanied by an enhanced fluorescence in intracellular compartments such as the ER (Fig. 7B). The diminished cell surface expression was corroborated by biotinylation (Fig. 7C). Furthermore, western blot analysis revealed that the ratio of mature to immature APP was drastically reduced for the mutants (Fig. 7C). All loop-S mutants were impaired in forming dimers, as shown by the diminished FRET efficiencies compared with the wild type (Fig. 7D). Note that one intact loop region is not sufficient to rescue the weakened dimerization, as shown by the coexpression of APP wild type with the loop-SD mutant. Thus, dimerization itself may be the signal for the plasma membrane localization. To investigate this assumption, we combined the loop-SD mutant with the L17C mutant, which encodes a previously described engineered disulfide-linked dimer (Munter et al., 2007). The loop-SD-L17C mutant could not rescue the impaired cell surface localization of APP. Thus, we conclude that the engineered dimerization per se is not a signal to induce trafficking of APP.

Discussion

At present, there is little information about mechanisms and functional consequences of APP and APLP homo- and heterophilic interactions. In this study we therefore analyzed these interactions by biochemical and biophysical techniques in living cells. The study revealed unique features of APLP1 within the APP protein family. As shown by confocal live-cell imaging, APLP2 and APP mainly localized to intracellular compartments, whereas APLP1 was found primarily at the cell surface. Additionally, upon coexpression, APP and APLP2 retained APLP1 in intracellular compartments, presumably by forming heteromeric complexes. As shown by

Journal of Cell Science

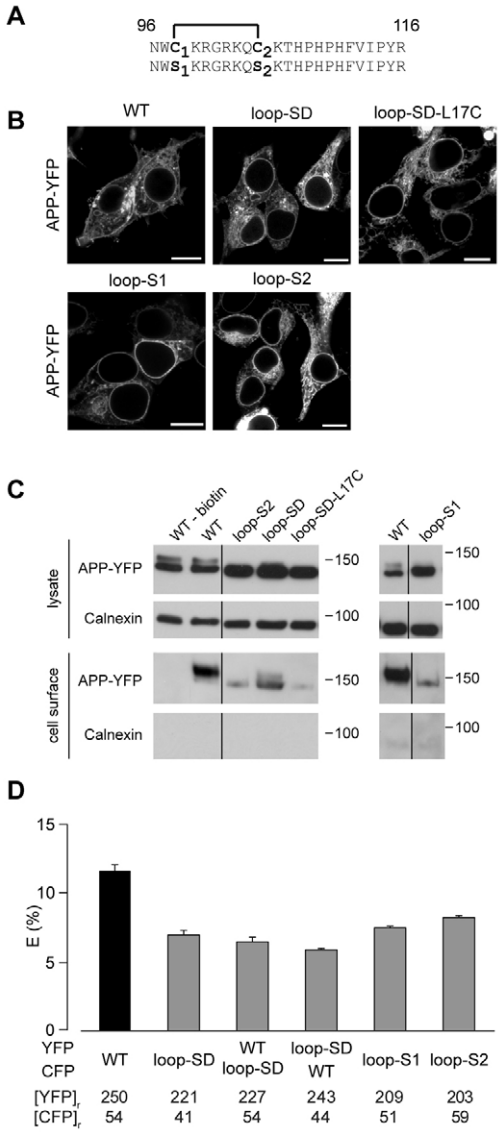

Fig. 7. Analysis of APP loop mutants. (A) Loop peptide sequence (amino acids 86 to 116 of the GFLD) with (wild type) and without (mutant sequence) the disulfide bridge. Single mutants are denoted with loop-S1 and loop-S2, and the double mutant with loop-SD. (B) Confocal imaging of APP loop mutants. YFP-tagged mutants were expressed in HEK293 cells and imaged by cLSM 1 day after transfection. Representative images of at least three independent transfections are shown. (C) Cell surface biotinylation of APP loop mutants. HEK293 cells were transiently transfected with the APP loop mutants and cell surface proteins were labeled by sulfo-NHS-SS-biotin, purified via neutravidin agarose and analyzed by western blot. Shown are western blots of the whole-cell lysates and the neutravidin eluate (cell surface). Molecular weight standards are indicated on the right. (D) FRET analysis of APP loop mutants. The mutant or WT YFP- and CFP-fusion proteins were expressed in HEK293 cells in different combinations and analyzed by FRET. Note that the presence of one loop is not sufficient to rescue the impaired dimerization (second bar versus third and fourth bar). The relative CFP and YFP fluorescence intensities in single cells expressing the respective fusion proteins were determined and averaged ($[YFP]_r$ and $[CFP]_r$) to verify comparable protein expression. Depicted are the means and s.e.m. of three to four independent transfections (with four measurements each on three to five cells). Bars, 10 μm. WT, wild type.

western blot analysis, this is not due to a reduced cell surface expression of APLP1, but rather an increase of total APLP1 protein levels. Potentially, retained APLP1 homodimers may be better substrates for degradation than APP:APLP1 or APLP2:APLP1 heterodimers, explaining the intracellular accumulation of APLP1 in the presence of APP or APLP2. Besides the retention of APLP1, endocytosis may be influenced by heterointeraction as previously suggested by others (Neumann et al., 2006). However, this is less likely, as APP homodimerization was shown to occur already in the ER (Scheuermann et al., 2001), and cell surface levels of APLP1 are increased relating to total protein levels. In the context of proposed receptor functions for the APP family proteins, changes in the level of cell surface expression may potentially influence accessibility to ligands and hence modulate signal transduction pathways by the APP or APLP intracellular domains (Leissring et al., 2002; Pardossi-Piquard et al., 2005). We could not test this hypothesis because such ligands that bind to APLP1 have not yet been identified. Additionally, the level of cell surface-localized APLP1 may also influence its ability to form trans interactions and thus affect cell-cell adhesion. Therefore, the heteromeric assembly of the APP family members possibly controls the function of the individual family members, rendering knowledge on the mechanisms of dimerization indispensable.

In accordance with the level of cell surface expression we show by cLSM, FRAP and co-immunoprecipitation analyses that solely APLP1 is capable of forming trans interactions in HEK293 cells. This is in disagreement with an initial study of the APP family in *Drosophila* Schneider cells (Soba et al., 2005), in which all family members were found to be involved in trans interactions. Although we cannot exclude that cell-type-specific differences are responsible for this disagreement, it is tempting to speculate that trans interactions of APLP1 exclusively occur via the GFLD region, whereas in APP and APLP2 this region is primarily engaged in cis dimerization. At least we cannot rule out that APP or APLP2 would also mediate trans interactions if they showed a similar cell surface localization to that of APLP1. Nevertheless, in HEK293 cells trans interactions were not observed for APP or APLP2. Additionally, only 5% of endogenous APP was detected at the cell surface in E15 embryonic mouse neurons (Brouillet et al., 1999), supporting the argument against an involvement of APP in cell-cell interactions in vivo.

APLP1, as well as APLP2, immunoreactivities in neuritic plaques significantly overlap with APP expression patterns, and the APP family proteins are processed by the same set of proteases (Bayer et al., 1997; Eggert et al., 2004; Gu et al., 2001; McNamara et al., 1998). Consequently, APP:APLP interactions may have particularly important implications for understanding cellular regulation and mechanisms of Aβ formation. By investigating the impact of APP:APLP coexpression on APP processing we observed no effect on α-secretase activity, as the sAPPα levels in the APP-overexpressing cells remained constant. This contradicts observations by Neumann et al., according to whom coexpression with APLP1 led to an increased shedding of APP by α-secretase (Neumann et al., 2006). Most likely these differences are due to the different cell types and different APP isoforms. Additionally, the alkaline phosphatase tag at the APP N-terminus may monomerize APP, as it was shown for GFP (Scheuermann et al., 2001).

Analysis of APP processing in APLP1 or APLP2 coexpressing cells revealed the production of toxic Aβ42 species to be more strongly affected than the Aβ40 levels. Based on the occurrence of heterodimerization and the concomitantly unimpaired production of secreted APP, we suggest that γ-secretase cleavage is affected. Recently we showed that the γ-cleavage site is determined by the

Journal of Cell Science

APP GxxxG motif of the transmembrane sequence, which mediates dimerization by helix-helix interactions (Munter et al., 2007). A disruption of this specific interaction diminished especially the Aβ42 generation. Thus, we postulate that in APP:APLP complexes Aβ levels are reduced by a natural disturbance of GxxxG helix-helix mediated interactions. So far, we have analyzed this in human neuroblastoma cells and cannot exclude that the situation might differ slightly in neurons. There is also the possibility that effects other than the heterodimerization are responsible for the diminished Aβ production. However, the fact that the Aβ42 levels specifically decreased supports the argument against a simple substrate competition for the secretases. In the light of our data, it is tempting to speculate that heterodimerization directly influences processing of APP to the toxic Aβ42 species, but the exact mechanism requires a further investigation on the level of substrate/secretase interactions.

Referring to the differences in co-localization and heterodimerization of APP:APLP1 compared to APP:APLP2, it seems remarkable that APLP1 and APLP2 have similar effects on Aβ generation. As the specific cellular site(s) of Aβ generation are still a matter of debate, we suggest that the co-localization of APP with APLP1 and APLP2, especially in intracellular compartments (e.g. endosomes) is sufficient to influence Aβ generation.

By creating N-terminal deletion mutants we could dissect the mechanisms of cis interactions in the APP protein family. The GFLD is crucial for cis-directed dimerization of APP and APLP2 but not of APLP1. By contrast, it was observed that the GFLD generated as a stable protease-resistant degradation product from APP18-350 per se is a monomer (Rossjohn et al., 1999). In addition, we recently demonstrated that residues in the copper-binding domain as well as the acidic region are important to mediate or stabilize dimerization (Kaden et al., 2008). This might explain why the crystallized fragment of APP (residues 18-123) was not found to form dimers.

Our data clearly show that deletion of the E1 domain in APLP1 leads only to an approximately 50% reduction of FRET efficiencies, demonstrating that dimerization is not fully inhibited by the lack of the E1 domain. Consequently, more C-terminal domains like the E2 domain contribute to the multimerization of APLP1 (Figs 5 and 6). This contradicts earlier published data suggesting that the E1 domain harbors the only contact site (Soba et al., 2005). An involvement of the conserved E2 domain is also supported by investigations showing that the E2 domain of APP reversibly dimerized in solution in an anti-parallel orientation (Wang and Ha, 2004). Importantly, our findings raise the interesting possibility that both E1 and E2 domains can mediate homo- and heterophilic interactions of APP family proteins in living cells. The contribution of each of the two domains resembles a double pan balance with more weight on the E1 site for APP and APLP2 and balanced or with even more weight on the E2 site for APLP1 (Fig. 8). In addition, the balance is further influenced by the acidic region, which has strong structural implications for APP homophilic interactions (Kaden et al., 2008).

The impact of the E1 domain, and especially of the GFLD region, for APP interactions was corroborated by mutants targeting the disulfide bridge between Cys 98 and Cys 105. The disruption of the disulfide bridge by a mutational approach had two effects. First, it impaired APP-APP interactions, and second, it diminished the cell surface localization of APP. Similar effects of conformational perturbations within secretory proteins have been described for chromogranin B and a muscle-specific kinase (Chanat et al., 1993; Gorr et al., 1999; Stiegler et al., 2006). However, the cell surface localization of the APP ΔGFLD mutant was not impaired, and thus we assume that structural changes or impaired folding in the GFLD, for example, are responsible for the effect of APP loop mutants. We cannot exclude the possibility that cysteine mutants other than those analyzed would have similar effects on APP cell surface localization and dimerization.

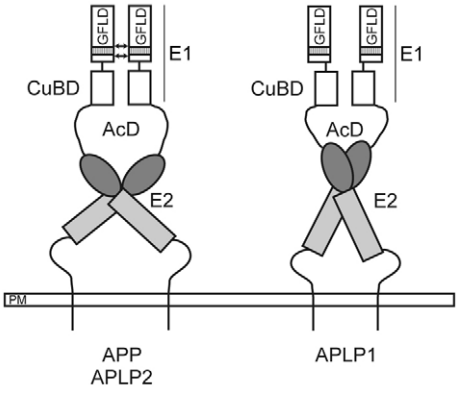

Fig. 8. Schematic representation of APP-, APLP2- and APLP1-cis dimerization. The E1 domain mediates homo- and heterophilic interactions of APP and APLP2 mainly through the GFLD, especially the loop region (striped square) as indicated by the arrows. By contrast, the GFLD is dispensable for dimerization of APLP1. The E2 domain of APLP1 substitutes the function of the E1 domain in initiating the interaction. However, for APP and APLP2 dimerization of the E1 domain is required to initiate the contact, which is stabilized by the E2 domain. The model of the E2 domain has been modified according to (Wang and Ha, 2004). PM, plasma membrane.

Recently, a proteomic approach using in vivo crosslinking revealed APLPs as interaction partners of APP (Bai et al., 2008). It is interesting to note that there might exist specific binding partners for all possible complexes as only one protein, the RasGAP-activating-like protein, for example, was identified as a binding partner for both APLP1 and APLP2, whereas a few other proteins were found that specifically interact with either APP, APLP1 or APLP2 (Bai et al., 2008).

In conclusion, this study uncovers a special role of APLP1 within the APP protein family regarding its subcellular localization, mechanisms of homo- and heterodimerization and the potential to mediate cell-cell interactions. Furthermore, the understanding of homo- and heterodimerization of APP and APLPs may lead to novel therapeutic approaches that are based on selectively promoting or disrupting certain heterodimer pairs to influence Aβ production. Additionally, the detailed knowledge of homo- and heterophilic interactions within the APP protein family offers new opportunities to identify as yet unknown ligands and will allow the dissection of specific APP and APLP functions.

Materials and Methods

Vectors and expression plasmids

Expression plasmids were generated by in-frame ligations of APLP1 and APLP2 cDNA in custom-made vectors pcDNA3-YFP, pcDNA3-CFP and pcDNA3-FLAG (Voigt et al., 2005). Generation of APP fusion vectors was done as previously described (Munter et al., 2007).

Generation of N-terminal deletion mutants: cDNAs coding for deletion mutants of APP, APLP1 and APLP2 were generated by a three-step PCR. The pcDNA3-YFP vectors coding for APP, APLP1 and APLP2 were used as templates. Primers designed for the generation of deletion mutants are listed in Table S1 of the supplementary material. Reverse primers were chosen so that internal restriction sites (*Xho*I for APP and *Eco*NI for APLP1 and APLP2) could be used for subsequent cloning. With the first forward primer, the N-terminus of the newly generated protein was defined and the signal sequence was added. With the second and third forward primers the signal sequence was elongated to the 5′ end. Additionally, with the third PCR a *Not*I

Journal of Cell Science

restriction site was introduced preceding the start codon for subcloning in the vectors pcDNA3-YFP-APP, -APLP1 and -APLP2. APP point mutations were introduced in the context of the YFP and CFP expression vectors by site-directed mutagenesis according to the manufacturer's protocol (Stratagene). Mutagenesis primers are listed in Table S1 of the supplementary material. All PCR and mutagenesis fragments were verified by didesoxy sequencing (GATC).

Cell culture

Cells were grown in an incubator at 37°C with 5% CO_2. Growth medium HEK293 cells: minimal essential medium (MEM, PAA), 10% fetal calf serum (FCS, PAA), 2 mM glutamine. Growth medium SH-SY5Y cells: Dulbecco's MEM/Ham's-F12 (Biochrom), 2 mM glutamine, 1× non-essential amino acids (PAA). For stable expression, medium was supplemented with 0.5 mg/ml G-418 sulfate (PAA) and 0.2 mg/ml Zeocin.

Confocal microscopy and fluorescence imaging

For confocal microscopy, an inverted confocal laser scanning microscope (LSM 510 Meta; Carl Zeiss) and an α-Plan-Fluor 100×/1.45 objective were used. Excitation and filter settings were used as described previously (Voigt et al., 2005). FRET efficiencies were determined using an acceptor photobleach protocol essentially as described in (Sinnecker et al., 2005; Voigt et al., 2005). Briefly, cells were excited at 410 and 515 nm for CFP and YFP detection, respectively. YFP was bleached at 512 nm for 2.1 seconds in each image acquisition cycle. To ensure appropriate conditions for FRET to occur, the relative CFP and YFP fluorescence intensities were determined and the molar ratio between coexpressed fluorescent acceptor and donor APLPs were adjusted to >0.8 (YFP:CFP) in all FRET experiments. For competition FRET experiments, the amounts of plasmids encoding fluorescent proteins were reduced to allow addition of up to 1 µg empty vector or plasmid encoding the non-fluorescent wild-type protein as a specific competitor. HEK293 cells were transiently transfected with plasmids encoding YFP and CFP fusions of APLP1, APLP2 and APP or the respective mutants using Fugene 6 transfection reagent (Roche Molecular Biochemicals) or transfectin (Bio-Rad Laboratories).

FRAP: a detailed description of the employed FRAP protocol will be published elsewhere (Tannert et al., 2008). Briefly, for monitoring the pre- and postbleach intensities, YFP was excited using the 458 nm line of an argon laser at low intensity passed through a 488 nm main beam splitter to further minimize bleaching. For bleach pulses, the 458, 488 and 514 nm lines of the argon laser were used at full output power. Before the bleach pulse, 10 prebleach images were recorded. The diffusion of fluorescent molecules into the bleached region from its surroundings was then monitored for 30 postbleach images. After an additional 40 s interval to ensure complete equilibration of the fluorescent molecules, the next bleach cycle was started. For each cell, the diffusion coefficient was given as the mean and s.e.m. of ten iteratively performed bleach cycles.

For data analysis, the pixel intensities were summed over the *y* dimension to obtain a one-dimensional intensity profile. To account for inhomogeneities in the distribution of the YFP-tagged protein, the postbleach intensity profiles were divided by the mean of the prebleach intensity profiles, thereby obtaining normalized intensities. One-dimensional diffusion coefficients were then calculated by simulating the diffusion along the membrane profile for variable diffusion coefficients until the best fit with the experimental data was obtained. To this end, a custom-made software using Brent's algorithm for the minimization was used.

The marker proteins (pEYFP-Golgi, pECFP-ER and pEYFPEndo from BD Biosciences Clontech) were used to determine the exact intracellular localization of the APP family proteins. Lysotracker red (DND-99, Molecular Probes, Invitrogen) was used to analyze lysosomal co-localization of the APP family proteins. YFP was detected as described before and the Lysotracker was excited by a 543 nm helium laser with 488/543 main beam splitter and detected via a 560 nm long-pass filter.

Immunofluorescence

Plasmids encoding APLP1, APLP2 and the empty vector (pcDNA3) were transiently transfected into HEK293 cells grown on glass cover slides. Cells were fixed with 4% paraformaldehyde and permeabilized with 0.3% Triton X-100 for 10 minutes. Cells were blocked with 1% BSA in PBS with 0.1% Tween for 1 hour followed by a 1 hour incubation with the first antibody. APLP1 was detected with polyclonal antiserum 42464, APLP2 with the new generated polyclonal antiserum 8-1 (see supplementary material Fig. S2). The secondary antibody was incubated for 45 minutes, i.e. goat anti-rabbit-Cy3. Finally, the nuclei were stained with 1× DAPI (Roche Molecular Biochemicals) for 10 minutes. Images were obtained using an LSM 510 meta (Carl Zeiss) confocal microscope. DAPI was excited at 364 nm and detected via a 385-470 nm band pass filter. Cy3 was excited at 543 nm and detected via a 560 nm long pass filter. Detection of YFP was carried out as already described (Voigt et al., 2005).

Immunoprecipitation and immunoblots

After co-transfection, cells were incubated for 24 hours, washed and lysed as previously described (Voigt et al., 2005). C-terminally FLAG-tagged proteins were immunoprecipitated by adding 4 µg anti-FLAG M2 monoclonal antibody (Sigma) and 30 µl protein G-Sepharose (GE Healthcare) and incubating overnight on a rotating shaker at 4°C. After centrifugation, protein G-Sepharose pellets were washed three times with high salt buffer (lysis buffer supplemented with 400 mM NaCl), followed by another washing step with lysis buffer and finally resuspended in gel loading buffer. For the trans co-immunoprecipitation the single transfected cells were replated and incubated for a further 24 hours, before immunoprecipitation was performed as described before. Samples were subjected to 8% SDS-PAGE and transferred to nitrocellulose membranes (Machery-Nagel GmbH & Co. KG, Düren, Germany). Immunodetection was performed using anti-FLAG M2 antibody (1:10,000) or antibodies specific for the respective protein, followed by probing with horseradish peroxidase-coupled anti-mouse (1:10,000) or anti-rabbit IgG antibodies (1:10,000; both Promega), respectively. Chemiluminescence was detected by ECL.

Cell surface biotinylation

HEK293 cells were transiently transfected with the APP and APLPs or APP loop mutants. Before biotinylation cells were washed three times with 37°C pre-warmed PBS supplemented with 0.5 mM $CaCl_2$ and 2 mM $MgCl_2$ (PBS^{++}). In order to empty the endocytic compartment, cells were incubated for 15 minutes in an incubator (37°C, 5% CO_2) in PBS^{++}. Cells were again rinsed with PBS^{++} and transferred to 4°C. EZ-Link sulfo-NHS-SS-biotin (Pierce) was added to a concentration of 0.25 mg/ml in ice-cold PBS^{++} and incubated for 15 minutes. After washing twice with ice-cold PBS^{++} the excess biotin was quenched with 5 mM glycine in PBS^{++} for 10 minutes. Cells were lysed and biotinylated proteins were purified by immobilized neutravidinbiotin binding protein agarose (Pierce). Agarose pellets were washed three times with stringent wash buffers (10 mM Tris, 150-500 mM NaCl, 0.2% NP-40, 2 mM EDTA) and eluted for 5 minutes at 95°C with reducing gel loading buffer, loaded on 8% Tris Glycin gels and analyzed by western blot.

Sandwich ELISA

Stably transfected SH-SY5Y cells were plated at a density of 4×10^5 cells per well of a twelve-well dish. The day after splitting, 500 µl of fresh media was added and incubated for 6 hours. For Aβ40- and Aβ42-specific ELISAs, 50 µl media was analyzed according to the manufacturer's instructions (The Genetics Company, Zürich, Switzerland). The same protocol was applied to determine sAPPα levels, except that an anti-Myc antibody (Cell Signaling Technology) was used. To determine total APP levels, cells of each well were lysed, and lysates were diluted 1:10 or 1:5 and analyzed by anti-Myc antibody.

Antibodies

The YFP fusion proteins in the trans co-immunoprecipitations were detected by a polyclonal GFP antibody (598, MBL Medical & Biological Laboratories Co., Japan). Calnexin was stained with a monoclonal antibody from Chemicon International. Immunodetection of APP was performed with the monoclonal W0-2 antibody (The Genetics Company, Zürich, Switzerland) (Ida et al., 1996). APLP1 was detected with the polyclonal 42464 antibody (Paliga et al., 1997). For detection of APLP2 we generated the polyclonal antibody 8/1. Rabbits were immunized with recombinant soluble sAPLP2α, purified from culture supernatants of sAPLP2α-expressing *Pichia pastoris* cells as described previously (Treiber et al., 2004). There was no cross-reactivity detected with other APP family proteins (shown in supplementary material Fig. S6).

We thank the DFG and BMBF for financial support and Ariane Schmechel for help with the production of polyclonal antibodies.

References

Atwood, C. S., Scarpa, R. C., Huang, X., Moir, R. D., Jones, W. D., Fairlie, D. P., Tanzi, R. E. and Bush, A. I. (2000). Characterization of copper interactions with alzheimer amyloid beta peptides: identification of an attomolaraffinity copper binding site on amyloid beta1-42. *J. Neurochem.* **75**, 1219-1233.

Bai, Y., Markham, K., Chen, F., Weerasekera, R., Watts, J., Horne, P., Wakutani, Y., Bagshaw, R., Mathews, P. M., Fraser, P. E. et al. (2008). The *in vivo* brain interactome of the amyloid precursor protein. *Mol. Cell Proteomics* **7**, 15-34.

Barnham, K. J., McKinstry, W. J., Multhaup, G., Galatis, D., Morton, C. J., Curtain, C. C., Williamson, N. A., White, A. R., Hinds, M. G., Norton, R. S. et al. (2003). Structure of the Alzheimer's disease amyloid precursor protein copper binding domain: a regulator of neuronal copper homeostasis. *J. Biol. Chem.* **278**, 17401-17407.

Bayer, T. A., Paliga, K., Weggen, S., Wiestler, O. D., Beyreuther, K. and Multhaup, G. (1997). Amyloid precursor-like protein 1 accumulates in neuritic plaques in Alzheimer's disease. *Acta Neuropathol.* **94**, 519-524.

Beher, D., Hesse, L., Masters, C. L. and Multhaup, G. (1996). Regulation of amyloid protein precursor (APP) binding to collagen and mapping of the binding sites on APP and collagen type I. *J. Biol. Chem.* **271**, 1613-1620.

Brouillet, E., Trembleau, A., Galanaud, D., Volovitch, M., Bouillot, C., Valenza, C., Prochiantz, A. and Allinquant, B. (1999). The amyloid precursor protein interacts with Go heterotrimeric protein within a cell compartment specialized in signal transduction. *J. Neurosci.* **19**, 1717-1727.

Brunkan, A. L. and Goate, A. M. (2005). Presenilin function and gamma-secretase activity. *J. Neurochem.* **93**, 769-792.

Cao, X. and Sudhof, T. C. (2001). A transcriptionally (correction of transcriptively) active complex of APP with Fe65 and histone acetyltransferase Tip60. *Science* **293**, 115-120.

Chanat, E., Weiss, U., Huttner, W. B. and Tooze, S. A. (1993). Reduction of the disulfide bond of chromogranin B (secretogranin I) in the trans-Golgi network causes its missorting to the constitutive secretory pathways. *EMBO J.* **12**, 2159-2168.

Chen, C. D., Oh, S. Y., Hinman, J. D. and Abraham, C. R. (2006). Visualization of APP dimerization and APP-Notch2 heterodimerization in living cells using bimolecular fluorescence complementation. *J. Neurochem.* **97**, 30-43.

Coulson, E. J., Barrett, G. L., Storey, E., Bartlett, P. F., Beyreuther, K. and Masters, C. L. (1997). Down-regulation of the amyloid protein precursor of Alzheimer's disease by antisense oligonucleotides reduces neuronal adhesion to specific substrata. *Brain Res.* **770**, 72-80.

Daigle, I. and Li, C. (1993). apl-1, a Caenorhabditis elegans gene encoding a protein related to the human beta-amyloid protein precursor. *Proc. Natl. Acad. Sci. USA* **90**, 12045-12049.

Eggert, S., Paliga, K., Soba, P., Evin, G., Masters, C. L., Weidemann, A. and Beyreuther, K. (2004). The proteolytic processing of the amyloid precursor protein gene family members APLP-1 and APLP-2 involves alpha-, beta-, gamma-, and epsilon-like cleavages: modulation of APLP-1 processing by n-glycosylation. *J. Biol. Chem.* **279**, 18146-18156.

Gorr, S. U., Huang, X. F., Cowley, D. J., Kuliawat, R. and Arvan, P. (1999). Disruption of disulfide bonds exhibits differential effects on trafficking of regulated secretory proteins. *Am. J. Physiol.* **277**, C121-C131.

Gu, Y., Misonou, H., Sato, T., Dohmae, N., Takio, K. and Ihara, Y. (2001). Distinct intramembrane cleavage of the beta-amyloid precursor protein family resembling gamma-secretase-like cleavage of Notch. *J. Biol. Chem.* **276**, 35235-35238.

Ida, N., Hartmann, T., Pantel, J., Schroder, J., Zerfass, R., Forstl, H., Sandbrink, R., Masters, C. L. and Beyreuther, K. (1996). Analysis of heterogeneous A4 peptides in human cerebrospinal fluid and blood by a newly developed sensitive Western blot assay. *J. Biol. Chem.* **271**, 22908-22914.

Kaden, D., Munter, L. M., Joshi, M., Treiber, C., Weise, C., Bethge, T., Voigt, P., Schaefer, M., Beyermann, M., Reif, B. et al. (2008). Homophilic interactions of the amyloid precursor protein (APP) ectodomain are regulated by the loop region and affect beta-secretase cleavage of APP. *J. Biol. Chem.* **283**, 7271-7279.

Leissring, M. A., Murphy, M. P., Mead, T. R., Akbari, Y., Sugarman, M. C., Jannatipour, M., Anliker, B., Muller, U., Saftig, P., De Strooper, B. et al. (2002). A physiologic signaling role for the gamma -secretase-derived intracellular fragment of APP. *Proc. Natl. Acad. Sci. USA* **99**, 4697-4702.

Li, Q. and Sudhof, T. C. (2004). Cleavage of amyloid-beta precursor protein and amyloid-beta precursor-like protein by BACE 1. *J. Biol. Chem.* **279**, 10542-10550.

McNamara, M. J., Ruff, C. T., Wasco, W., Tanzi, R. E., Thinakaran, G. and Hyman, B. T. (1998). Immunohistochemical and in situ analysis of amyloid precursor-like protein-1 and amyloid precursor-like protein-2 expression in Alzheimer disease and aged control brains. *Brain Res.* **804**, 45-51.

Munter, L. M., Voigt, P., Harmeier, A., Kaden, D., Gottschalk, K. E., Weise, C., Pipkorn, R., Schaefer, M., Langosch, D. and Multhaup, G. (2007). GxxxG motifs within the amyloid precursor protein transmembrane sequence are critical for the etiology of Abeta42. *EMBO J.* **26**, 1702-1712.

Neumann, S., Schobel, S., Jager, S., Trautwein, A., Haass, C., Pietrzik, C. U. and Lichtenthaler, S. F. (2006). Amyloid precursor-like protein 1 influences endocytosis and proteolytic processing of the amyloid precursor protein. *J. Biol. Chem.* **281**, 7583-7594.

Nishimoto, I., Okamoto, T., Matsuura, Y., Takahashi, S., Okamoto, T., Murayama, Y. and Ogata, E. (1993). Alzheimer amyloid protein precursor complexes with brain GTP-binding protein G(o). *Nature* **362**, 75-79.

Nyborg, A. C., Ladd, T. B., Zwizinski, C. W., Lah, J. J. and Golde, T. E. (2006). Sortilin, SorCS1b, and SorLA Vps10p sorting receptors, are novel gamma-secretase substrates. *Mol. Neurodegener.* **1**, 3.

Paliga, K., Peraus, G., Kreger, S., Durrwang, U., Hesse, L., Multhaup, G., Masters, C. L., Beyreuther, K. and Weidemann, A. (1997). Human amyloid precursor-like protein 1-cDNA cloning, ectopic expression in COS-7 cells and identification of soluble forms in the cerebrospinal fluid. *Eur. J. Biochem.* **250**, 354-363.

Pardossi-Piquard, R., Petit, A., Kawarai, T., Sunyach, C., Alves da Costa, C., Vincent, B., Ring, S., D'Adamio, L., Shen, J., Muller, U. et al. (2005). Presenilin-dependent transcriptional control of the Abeta-degrading enzyme neprilysin by intracellular domains of betaAPP and APLP. *Neuron* **46**, 541-554.

Pastorino, L., Ikin, A. F., Lamprianou, S., Vacaresse, N., Revelli, J. P., Platt, K., Paganetti, P., Mathews, P. M., Harroch, S. and Buxbaum, J. D. (2004). BACE (beta-secretase) modulates the processing of APLP2 *in vivo*. *Mol. Cell Neurosci.* **25**, 642-649.

Rosen, D. R., Martin-Morris, L., Luo, L. Q. and White, K. (1989). A Drosophila gene encoding a protein resembling the human beta-amyloid protein precursor. *Proc. Natl. Acad. Sci. USA* **86**, 2478-2482.

Rossjohn, J., Cappai, R., Feil, S. C., Henry, A., McKinstry, W. J., Galatis, D., Hesse, L., Multhaup, G., Beyreuther, K., Masters, C. L. et al. (1999). Crystal structure of the N-terminal, growth factor-like domain of Alzheimer amyloid precursor protein. *Nat. Struct. Biol.* **6**, 327-331.

Scheinfeld, M. H., Ghersi, E., Laky, K., Fowlkes, B. J. and D'Adamio, L. (2002). Processing of beta-amyloid precursor-like protein-1 and -2 by gamma-secretase regulates transcription. *J. Biol. Chem.* **277**, 44195-44201.

Scheuermann, S., Hambsch, B., Hesse, L., Stumm, J., Schmidt, C., Beher, D., Bayer, T. A., Beyreuther, K. and Multhaup, G. (2001). Homodimerization of amyloid precursor protein and its implication in the amyloidogenic pathway of Alzheimer's disease. *J. Biol. Chem.* **276**, 33923-33929.

Shivers, B. D., Hilbich, C., Multhaup, G., Salbaum, M., Beyreuther, K. and Seeburg, P. H. (1988). Alzheimer's disease amyloidogenic glycoprotein: expression pattern in rat brain suggests a role in cell contact. *EMBO J.* **7**, 1365-1370.

Sinnecker, D., Voigt, P., Hellwig, N. and Schaefer, M. (2005). Reversible photobleaching of enhanced green fluorescent proteins. *Biochemistry* **44**, 7085-7094.

Small, D. H., Nurcombe, V., Reed, G., Clarris, H., Moir, R., Beyreuther, K. and Masters, C. L. (1994). A heparin-binding domain in the amyloid protein precursor of Alzheimer's disease is involved in the regulation of neurite outgrowth. *J. Neurosci.* **14**, 2117-2127.

Soba, P., Eggert, S., Wagner, K., Zentgraf, H., Siehl, K., Kreger, S., Lower, A., Langer, A., Merdes, G., Paro, R. et al. (2005). Homo- and heterodimerization of APP family members promotes intercellular adhesion. *EMBO J.* **24**, 3624-3634.

Stiegler, A. L., Burden, S. J. and Hubbard, S. R. (2006). Crystal structure of the agrin-responsive immunoglobulin-like domains 1 and 2 of the receptor tyrosine kinase MuSK. *J. Mol. Biol.* **364**, 424-433.

Storey, E., Beyreuther, K. and Masters, C. L. (1996). Alzheimer's disease amyloid precursor protein on the surface of cortical neurons in primary culture co-localizes with adhesion patch components. *Brain Res.* **735**, 217-231.

Tannert, A., Voigt, P., Burgold, S., Tannert, S. and Schaefer, M. (2008). Signal amplification between G beta gamma release and PI3K gamma-mediated PI(3,4,5)P3 formation monitored by a fluorescent G beta gamma biosensor protein and repetitive two component total internal reflection/fluorescence redistribution after photobleachung analysis. *Biochemistry* **47**, 11239-11250.

Treiber, C., Simons, A., Strauss, M., Hafner, M., Cappai, R., Bayer, T. A. and Multhaup, G. (2004). Clioquinol mediates copper uptake and counteracts copper efflux activities of the amyloid precursor protein of Alzheimer's disease. *J. Biol. Chem.* **279**, 51958-51964.

Voigt, P., Brock, C., Nürnberg, B. and Schaefer, M. (2005). Assigning functional domains within the p101 regulatory subunit of phosphoinositide 3-kinase gamma. *J. Biol. Chem.* **280**, 5121-5127.

Walsh, D. M., Fadeeva, J. V., LaVoie, M. J., Paliga, K., Eggert, S., Kimberly, W. T., Wasco, W. and Selkoe, D. J. (2003). gamma-Secretase cleavage and binding to FE65 regulate the nuclear translocation of the intracellular C-terminal domain (ICD) of the APP family of proteins. *Biochemistry* **42**, 6664-6673.

Wang, Y. and Ha, Y. (2004). The X-ray structure of an antiparallel dimer of the human amyloid precursor protein E2 domain. *Mol. Cell* **15**, 343-353.

Wasco, W., Bupp, K., Magendantz, M., Gusella, J. F., Tanzi, R. E. and Solomon, F. (1992). Identification of a mouse brain cDNA that encodes a protein related to the Alzheimer disease-associated amyloid beta protein precursor. *Proc. Natl. Acad. Sci. USA* **89**, 10758-10762.

Wasco, W., Gurubhagavatula, S., Paradis, M. D., Romano, D. M., Sisodia, S. S., Hyman, B. T., Neve, R. L. and Tanzi, R. E. (1993). Isolation and characterization of APLP2 encoding a homologue of the Alzheimer's associated amyloid beta protein precursor. *Nat. Genet.* **5**, 95-100.

Journal of Cell Science